ELSEVIER

Surface Science 400 (1998) 11–18

surface science

Coverage dependence of neopentane trapping dynamics on Pt(111)

J.F. Weaver, K.L. Ho, M.A. Krzyzowski, Robert J. Madix *

Department of Chemical Engineering, Stanford University, Stanford, CA 94305, USA

Received 19 August 1997; accepted for publication 21 October 1997

Abstract

Adsorption probabilities for neopentane on Pt(111) were measured directly using supersonic molecular-beam techniques at coverages ranging from zero to monolayer saturation, incident translational energies between 18 and 110 kJ mol^{-1} and incident angles between 0° and 60° at a surface temperature of 105 K. The adsorption probability was found to increase with coverage up to near monolayer saturation at all incident translational energies and incident angles. The coverage dependence of the adsorption probability predicted by a modified Kisliuk model with enhanced trapping into the second layer exhibits good quantitative agreement with the experimental values. The angular dependence of the adsorption probability decreases with increasing coverage, suggesting that the effective corrugation of the gas–surface interaction potential increases with the adsorbate coverage. The initial adsorption probability into the second layer onto the covered surface decreases from 0.95 to 0.75 with increasing energy over the energy range studied, and exhibits total energy scaling. A comparison with second-layer trapping data of simpler molecules onto covered Pt(111) indicates that the structural complexity of adsorbed neopentane molecules facilitates collisional energy transfer during adsorption.

Keywords: Adsorption kinetics; Alkanes; Low index single crystal surfaces; Molecular dynamics; Molecule–solid scattering and diffraction – inelastic

1. Introduction

In industrial catalytic processes, most phenomena at the gas–surface interface occur on surfaces which are at least partially covered by adsorbates, which can have a strong influence on both the kinetics [1–5] and dynamics of adsorption. Supersonic molecular-beam techniques are a powerful probe of the effects which adsorbed molecules have on adsorption; however, only a few molecular-beam investigations have been conducted to investigate dynamical effects on adsorbate-covered surfaces [6–16]. In the few studies reported, it is generally observed that adsorbed molecules or molecular fragments increase the adsorption probability over that of the clean surface. This decidedly ''anti-Langmuirian'' and ''non-Kisliukian'' behavior is of considerable interest, suggesting that adsorbed intermediates can actually promote adsorption into a molecular precursor state and enhance adsorption. In this study, we have extended our studies of adsorbate-induced adsorption of alkanes [7,8,12] using supersonic molecular beams to investigate the coverage dependence of the trapping probability of neopentane on Pt(111). We chose to study the adsorption

* Corresponding author. Tel: (+1) 650 7232402; Fax: (+1) 650 7239780; e-mail: rjm@rio.stanford.edu.

0039-6028/98/$19.00
PII S0039-6028(97)00836-4

dynamics of a large alkane with a higher molecular weight than those investigated previously to determine the effects of molecular weight and size on the fundamental mechanisms governing alkane adsorption.

Numerous models have been proposed to describe the adsorption dynamics on covered surfaces. The Langmuir site-exclusion principle stipulates that a molecule impinging on an occupied site on the surface is reflected, while a molecule impinging on an unoccupied site is adsorbed with probability S_0. Therefore, the adsorption probability at the covered surface is a linearly decreasing function of coverage

$$S(\theta)=S_0(1-\theta), \tag{1}$$

where S is the adsorption probability, S_0 is the adsorption probability at zero coverage and θ is the fractional coverage of the first monolayer.

Early experiments on carbon monoxide adsorption on metals showed S to be independent of coverage at low temperature, and prompted Kisliuk to propose a model which involves weakly bound precursor states in the adsorption process [2]. In the Kisliuk model, adsorption on the clean surface occurs through intrinsic precursor-mediated adsorption which entails the trapping of molecules into weakly bound states over unoccupied sites prior to adsorption. In addition, extrinsic precursors form at non-zero coverage as weakly bound, mobile species above occupied sites which can migrate to clean surface sites and become trapped as intrinsic precursors. A kinetic representation for the Kisliuk model for molecular adsorption is

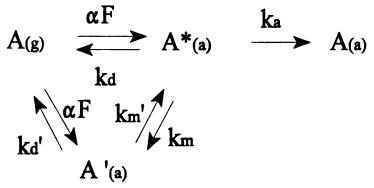

where F is the incident flux in monolayers per se and intrinsic and extrinsic precursors are represented by * and ′, respectively. In the steady state, the coverage dependence of S is given by

$$S(\theta)=\frac{S_0}{1+[\theta/(1-\theta)]K}, \tag{2}$$

where

$$K=\left(\frac{k_a+k_d+k_m}{k_a+k_d}\right)\left(\frac{k'_d}{k'_m+k'_d}\right). \tag{3}$$

The Kisliuk model predicts that the adsorption probability $S(\theta)$ is equal to S_0 at submonolayer coverage and decreases to zero at saturation coverage. Furthermore, according to the model, the adsorption probability always decreases with coverage. For CO adsorption on Ni(100), transitions from Kisliukian to Langmuirian behavior occur with increasing kinetic energy of the incident gas [13]. However, as noted above, in some cases the adsorption probability actually increases with coverage [3,6–10].

As a result, a model with enhanced trapping into the second layer was proposed for systems in which the adsorption probability increases with surface coverage [6,7,10]. In this model, adsorption occurs either directly or through extrinsic precursors. The molecules trapped on the occupied sites can migrate towards the unoccupied sites and adsorb. The steps in this model are given by

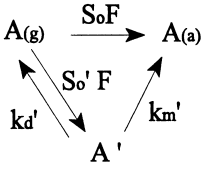

where S_0 is the adsorption probability at zero coverage and S'_0 is taken to be the adsorption probability at the saturation of the first monolayer. The coverage dependence of the trapping probability according to this representation is given by

$$S(\theta)=S_0(1-\theta)+\frac{S'_0(1-\theta)q_m\theta}{(1-q_m\theta)}, \tag{4}$$

where

$$q_m=\frac{k'_m}{k'_m+k'_d}. \tag{5}$$

When $k'_m \gg k'_d$, q_m approaches unity and Eq. (4) becomes the simple relationship

$$S(\theta) = S_0(1-\theta) + S'_0\theta. \quad (6)$$

In this limit, all molecules adsorbed on the second layer remain adsorbed, and when S'_0 is greater than S_0, $S(\theta)$ increases with θ. The adsorption of ethane [6] onto Ir(110) and ethane [7], propane [8] and xenon [10] onto Pt(111) are accurately reproduced by this simple expression. Moreover, recent dynamical simulations reveal that the mechanisms for adsorbate-assisted adsorption of xenon on Pt(111) are well represented in the modified Kisliuk model [17].

In this supersonic molecular-beam study, we measured the molecular adsorption probability of neopentane on Pt(111) as a function of incident translational energy, angle and neopentane coverage at a surface temperature of 105 K. At all incident conditions, the neopentane trapping probabilities increase with increasing coverage, and are described well by the modified Kisliuk model. The adsorption probability exhibits a decreasing dependence on the incident angle as the neopentane coverage increases, reaching total energy scaling at monolayer saturation coverage. The behavior qualitatively mimics that of both ethane and propane adsorption on Pt(111), although the trapping probability of neopentane is higher.

2. Experimental

The molecular-beam scattering apparatus employed in this study has been described in detail previously [18,19]. Briefly, the apparatus consists of an ultrahigh vacuum (UHV) scattering chamber with a typical base pressure of $\leq 1 \times 10^{-10}$ Torr coupled to a triply differentially pumped supersonic molecular-beam source. Neopentane molecular beams were generated in the first chamber by expansion through a nozzle with an aperture diameter of 55 ± 5 μm. The second stage of the beam source contains a mechanical chopper assembly with a 50% duty cycle to modulate the beam and a solenoid-activated shutter to block or allow passage of the beam into the main scattering chamber. A moveable, non-adsorbing flag was located in the UHV scattering chamber along the beam line and was used to prevent the beam from directly striking the Pt(111) crystal, which was mounted in the center of the scattering chamber. The UHV chamber contained a retarding field analyzer (RFA) for Auger electron spectroscopy (AES) and low-energy electron diffraction (LEED) as well as two mass spectrometers: (i) a "stationary" mass spectrometer mounted on a bellows which was used primarily for direct sticking probability (DSP) and temperature-programmed desorption (TPD) experiments, and (ii) a rotatable mass spectrometer which moves at a fixed distance of 10.5 cm about the sample and was used to measure beam translational energies.

All experiments were performed on a clean Pt(111) surface which produced the expected p(1 × 1) hexagonal LEED pattern. Initial cleaning procedures consisted of cycles of Ar^+ sputtering and annealing to temperatures >1300 K followed by standard oxygen titration procedures to remove carbonaceous residues. Surface temperatures were measured using a chromel–alumel thermocouple spot-welded to the back of the crystal. The primary contaminants which were observed initially were calcium and carbon. Once the calcium impurity was removed by sputtering, only oxygen cleaning was routinely used to remove carbon contamination. Sputtering was only occasionally necessary to remove calcium which migrated to the surface from the bulk. When impurity concentrations were less than the sensitivity of AES (<0.01 ML), the surface was assumed to be clean.

Neopentane translational energies were varied from 18 to 110 kJ mol^{-1} by seeding neopentane into either argon or helium. The nozzle temperature was kept constant at 310 ± 3 K to minimize variations in the internal energy of neopentane. Translational energies were measured by modulating the beam at frequencies near 650 Hz and monitoring the most abundant cracking fragment of neopentane ($m/q = 57$) at the front and back of the chamber using the rotatable mass spectrometer in a phase-sensitive detection mode. The phase difference between the signals detected was used to calculate the neopentane flight time across the chamber. Neopentane partial pressures were kept as low as possible to inhibit cluster formation in

the nozzle, since aggregation has been observed for other molecules and atoms expanding out of nozzles at room temperature under slightly higher stagnation pressures [20–22]. To test for neopentane dimers, the beam was directed into the rotatable mass spectrometer. The mass spectrometer sensitivity to dimers was maximized by reducing the ionizer electron energy to less than 20 eV and by increasing the multiplier gain [23]. No neopentane clusters were observed for a nozzle temperature of 310 K and the highest neopentane partial pressures ($\sim$0.4 bar) used in forming the beams.

The trapping probability of neopentane as a function of neopentane coverage was measured directly with the stationary mass spectrometer using the reflectivity method of King and Wells [24]. All of the experiments were conducted at a surface temperature of 105 K. Fig. 1 illustrates the direct method for determining the coverage-dependent adsorption probabilities on an initially clean surface. Initially, the neopentane beam was blocked from entering the scattering chamber by the solenoid-activated shutter. After 20 s the shutter was opened, allowing the beam to enter the chamber and strike the inert flag. A reference background partial pressure ($P1$) of neopentane was produced when the beam struck the flag since the neopentane does not adsorb on the gold-plated surface. At 40 s, the flag was abruptly removed from in front of the crystal, causing a transient decrease in the $(CH_3)_4C$ partial pressure ($P2$) due to adsorption onto the Pt(111) surface. The ratio of the initial transient partial pressure decrease to the reference background partial pressure increase, $P2/P1$, provides an absolute measurement of the adsorption probability in the zero-coverage limit S_0. Following the initial abrupt decrease, the partial pressure continued to decrease almost linearly to point D, which corresponds to saturation of the neopentane monolayer (see below). At a particular fractional coverage, say point E, the adsorption probability is given by the ratio $P3/P1$ at the corresponding fractional coverage given by the area ratio ABEF/ACDF. The uncertainty in the fractional coverage determined by the method of King and Wells is estimated to be about ± 0.01 for these measurements. In the experiment shown in Fig. 1, the exposure was terminated at 60 s by repositioning the flag to block the beam. The neopentane partial pressure in the UHV scattering chamber was measured by monitoring the intensity of the most abundant neopentane ion ($m/q=57$). The accuracy in the measured adsorption probability is about ± 0.02 for these experiments.

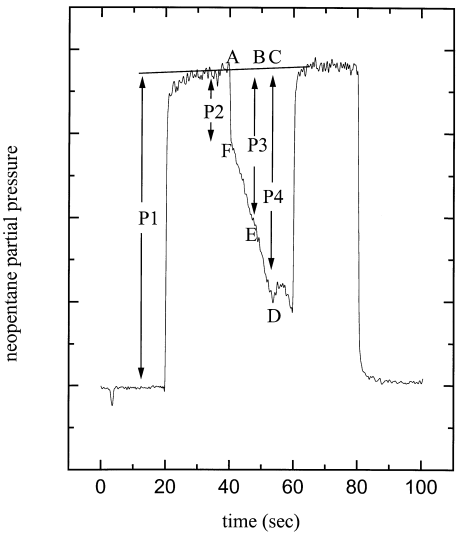

Fig. 1. Example data curve of the direct method to measure the initial adsorption probability onto the clean surface, the adsorption probability as a function of coverage and the initial adsorption probability into the second layer. See text for explanation.

TPD experiments indicate that molecular neopentane desorbs from the monolayer state on Pt(111) at 200 K, and that multilayer desorption occurs near 125 K. We verified that the abrupt change in the neopentane partial pressure after continued beam exposure (point D in Fig. 1) was indeed due to saturation of the monolayer. This was accomplished by repeating an adsorption experiment at increasing surface temperatures, causing the rate of desorption from the second layer state to also increase in an observable manner. For surface temperatures up to 140 K, the time profile of the partial pressure trace was unaffected by the temperature change from the time of the initial exposure to point D. At point D, the partial pressure rose to increasingly higher values as the surface temperature was increased, due to the commencement of desorption from the surface at that coverage. Similar behavior has been noted previously for ethane and propane adsorp-

tion on Pt(111). We take this point to indicate saturation of the monolayer and use it to evaluate the initial adsorption probability into the extrinsic precursor state S_0'. Indeed, if the surface is re-exposed to the beam after completion of the experiment shown in Fig. 1 at a surface temperature of about 110 K, the partial pressure trace repeats exactly, starting at point D.

3. Results and discussion

3.1. Molecular versus dissociative adsorption

The dissociation of molecularly adsorbed neopentane occurs with very low probability, if at all, on Pt(111) terrace sites [25]. Consistent with these findings, RAIRS (reflection–absorption infrared spectroscopy) indicates that neopentane adsorbs molecularly on Pt(111) at 150 K [26]. However, molecularly adsorbed neopentane does dissociate at surface defect sites on Pt(111) over the surface temperature range of 300–800 K. Since defect sites constitute only a small fraction of the surface, most neopentane molecules incident with low translational energies ($\leq$110 kJ mol^{-1}) adsorb into a reversible molecular state on Pt(111).

To test whether neopentane dissociating on the surface influenced our trapping measurements, we frequently performed the following procedure. After adsorption at 105 K the surface was quickly heated to desorb neopentane, cooled back down to 105 K and then the uptake experiment was repeated. In all cases, the molecular adsorption probability remained the same within the experimental error over a wide range of neopentane incident energies and angles. Based on this observation and the RAIRS results, we conclude that dissociative adsorption of neopentane was not a significant effect in our measurements of the trapping probability at 105 K.

3.2. Trapping dynamics on clean Pt(111)

The initial trapping probabilities of neopentane on clean Pt(111) at 105 K scale with $E_i \cos^{0.6}\theta_i$ for neopentane incident energies E_i from 18 to 110 kJ mol^{-1} and incident angles θ_i from 0 to 60°, where θ_i is the angle measured from the surface normal (Fig. 2). The decrease in the adsorption probability as the incident energy is increased is expected for non-activated molecular trapping, since a larger fraction of energy must be dissipated to the surface or internal motions for the molecule to become trapped in the potential well. Both ethane [27] and propane [8] trapping on Pt(111) also exhibit $n=0.6$ energy scaling. The angular dependence of the trapping probabilities, as specified by the $E_i \cos^{0.6}\theta_i$ energy scaling, suggests that dissipation of the momentum component directed along the surface normal is more important than parallel momentum exchange in facilitating neopentane trapping. However, the low value of the scaling exponent (0.6) suggests that parallel momentum participates in the trapping process through the collisional interchange of normal and parallel momenta, which results from corrugation of the gas–surface interaction. Indeed, trajectory calculations reveal that a periodic variation in the

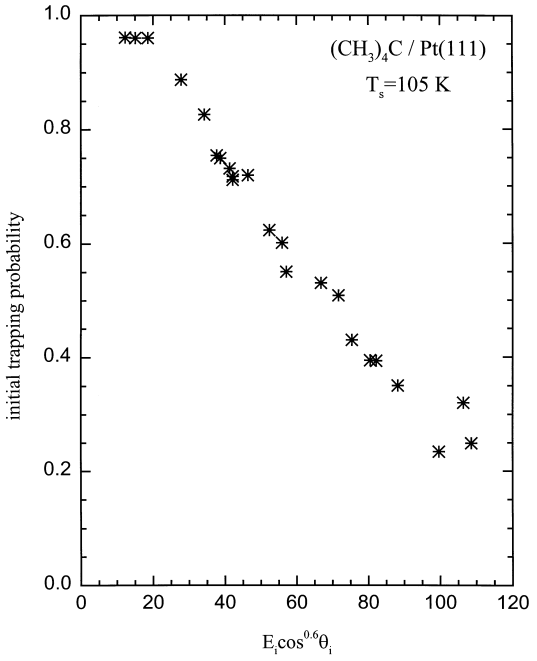

Fig. 2. Initial adsorption probabilities of neopentane onto clean Pt(111) as a function of the energy scaling function $E_i \cos^{0.6}\theta_i$ for incident energies, E_i, ranging from 18 to 110 kJ/mol and incident angles θ_i, from 0 to 60°. The surface temperature was constant at 105 K.

gas–surface interaction potential is responsible for the non-normal energy scaling of ethane [28,30] and propane [29,30] on Pt(111). Hence, the dynamics governing neopentane trapping on clean Pt(111) also appear to be influenced by corrugation in the potential between the molecule and surface.

3.3. Coverage dependence of the adsorption probability

For all incident energies and angles, the molecular adsorption probability of neopentane increases with increasing coverage, and hence cannot be represented well by either Langmuirian kinetics or the original Kisliuk model. The modified Kisliuk model accurately represents the dependence of the adsorption probability (S) on coverage (θ), as was observed for the coverage-dependent trapping probabilities of ethane [7] and propane [8] on Pt(111) (Fig. 3). The fact that the value of q_m is close to 1 indicates that the desorption rate from the extrinsic precursor state is negligible in comparison with the rate of migration of species adsorbed in the extrinsic precursor state. As discussed in Section 2, the values of S_0' which were used in the fits were computed directly from the experimental data without adjustment.

The coverage-dependent adsorption probability of neopentane on Pt(111) also becomes less sensitive to the incident angle as coverage increases (Fig. 4), with $S(\theta)$ exhibiting total energy scaling at coverages of 0.7 and higher. This trend has been previously attributed to an increase in the effective corrugation of the gas–surface potential with increasing coverage. Recent trajectory calculations of ethane trapping onto sulfur-covered Pt(111) also reveal that an increase in the static surface

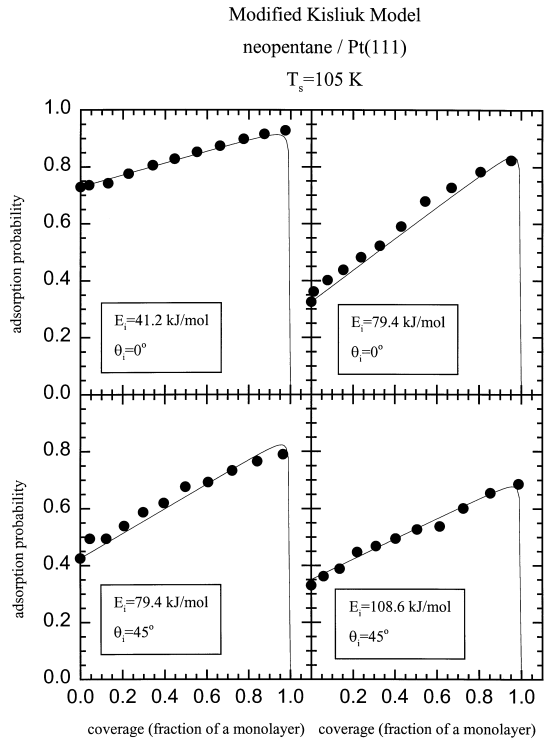

Fig. 3. Four figures showing the dependence of the adsorption probability on neopentane coverage for various incident translational energies and incident angles. The solid circles indicate the experimental data and the solid lines indicate the results calculated using the modified Kisliuk model with a value of $q_m = 0.999$.

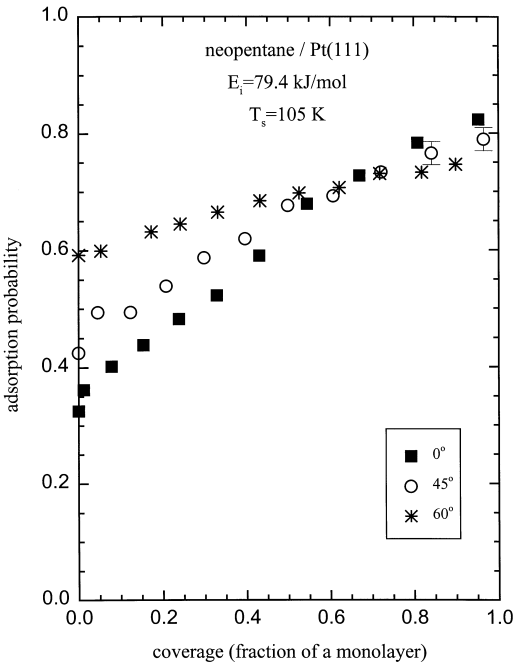

Fig. 4. Molecular adsorption probability as a function of coverage for three different incident angles, 0, 45 and 60°, at an incident energy of 79.4 kJ mol^{-1} and at a surface temperature of 105 K. The adsorption probability becomes progressively less sensitive to the incident angle as the coverage increases.

corrugation relative to the clean surface causes the adsorption probabilities to be angularly independent [31]. Except at the highest kinetic energy, there is little effect of incident angle on the initial adsorption probability of neopentane onto the monolayer (Fig. 5). The slight angular dependence at high kinetic energies most probably results from the onset of direct dissociation [25], which would contribute a small, angularly dependent factor to the overall adsorption probability as measured by the method of King and Wells. Subtracting the direct dissociation probability from the measured second-layer adsorption probability at 108.6 kJ mol^{-1} results in a more angularly independent curve, as expected based on the low-energy results.

The increase of $S(\theta)$ with increasing neopentane coverage indicates that adsorbed neopentane facilitates the dissipation of collisional energy during neopentane adsorption. Enhanced energy transfer might be expected on the adsorbate-covered surface due to the favorable match in mass of the collision partners. However, both molecular-beam data and dynamical calculations demonstrate that factors such as corrugation and adsorbate structure can dominate the adsorption dynamics on covered surfaces [7,8,12,31]. For example, for nearly equivalent mass ratios of ethane and each adsorbate, ethane trapping increased as the adsorbate complexity increased (ethane > ethylidyne > sulfur) [12]. Fig. 6 also shows that the trapping probabilities of molecules onto their adsorbed counterparts on Pt(111) (second-layer adsorption) are highest for neopentane and decrease in the order $C_3H_8 > C_2H_6 >$ xenon. Indeed, as the structural complexity of the adsorbate increases, so do the internal degrees of freedom available for collisional energy transfer. It is notable that the adsorption probability of neopentane into the extrinsic precursor state is substantially higher than that of both propane and ethane. This suggests that low-frequency

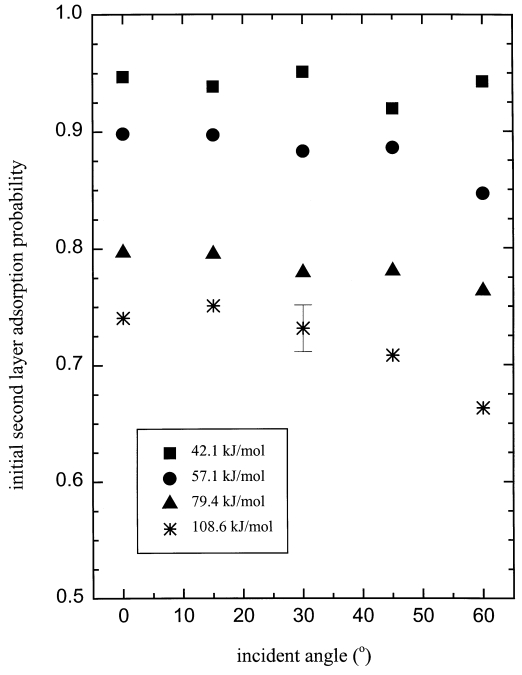

Fig. 5. Initial adsorption probability onto a monolayer of adsorbed neopentane as a function of incident angle for four different incident translational energies and at a surface temperature of 105 K. Note that the second layer adsorption probability is insensitive to the incident angle. The error bars represent an uncertainty of ± 0.02 in the measured adsorption probabilities.

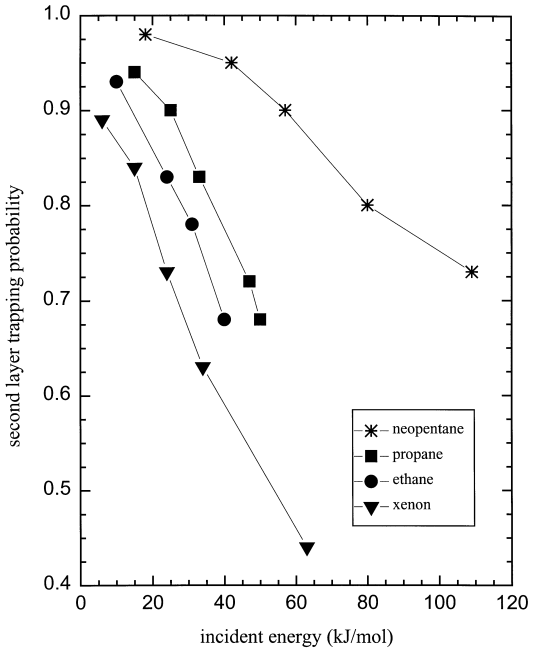

Fig. 6. Second-layer adsorption probability at normal incidence as a function of incident translational energy. Data for ethane, propane and xenon were taken from Refs. [7,8,10], respectively.

skeletal deformations may contribute significantly to energy dissipation in these collisions.

4. Conclusions

The general characteristics of the coverage-dependent trapping dynamics of neopentane on Pt(111) are identical to those for previously investigated molecules on this surface. The increase in the adsorption probability with increasing neopentane coverage is well described by a modified Kisliuk model with enhanced trapping into the second layer. In addition, it is observed that parallel momentum participates in the collisional energy transfer at all neopentane coverages and becomes increasingly important as coverage increases, suggesting a high effective corrugation of the gas–surface potential for the covered surface. Perhaps more importantly, however, this study demonstrates that trapping into the extrinsic precursor state is significantly enhanced as the adsorbate complexity increases. This observation suggests that collisional energy transfer on covered surfaces may involve substantial internal mode excitation of the adsorbed species which significantly promotes adsorption. Therefore, adsorbate molecular structure must be carefully considered in a dynamical description of trapping onto covered surfaces.

Acknowledgements

Financial support for this work was provided by the Department of Energy, Chemical Sciences Division, Office of Basic Energy Sciences (grant DE-FGO3-86ER13468).

References

[1] G. Ehrlich, J. Phys. Chem. 59 (1955) 473.
[2] P. Kisliuk, J. Chem. Phys. Solids 3 (1957) 95.
[3] M. Bowker, D.A. King, J. Chem. Soc., Faraday Trans. 75 (1979) 2100.
[4] D. Menzel, in: M. Grunze, M. Kreuzer (Eds.), Kinetics of Interface Reactions, Springer, Berlin, 1987.
[5] W.H. Weinberg in: M. Grunze, M. Kreuzer (Eds.), Kinetics of Interface Reactions, Springer, Berlin, 1987.
[6] H.C. Kang, C.B. Mullins, W.H. Weinberg, J. Vac. Sci. Technol. A 8 (1990) 2538.
[7] C.R. Arumainayagam, M.C. McMaster, R.J. Madix, J. Phys. Chem. 95 (1991) 2461.
[8] M.C. McMaster, C.R. Arumainayagam, R.J. Madix, Chem. Phys. 177 (1993) 461.
[9] M.C. McMaster, S.L.M. Schroeder, R.J. Madix, Surf. Sci. 297 (1993) 253.
[10] C.R. Arumainayagam, J.A. Stinnett, M.C. McMaster, R.J. Madix, J. Chem. Phys. 95 (1991) 5437.
[11] S.A. Soulen, J.A. Stinnett, R.J. Madix, Surf. Sci. 303 (1994) 312.
[12] J.A. Stinnett, M.C. McMaster, R.J. Madix, Surf. Sci. 364 (1996) 325.
[13] M.P. D'Evelyn, H.-P. Steinruck, R.J. Madix, Surf. Sci. 180 (1987) 47.
[14] D. Kelly, W. Hago, W.H. Weinberg, J. Vac. Sci. Technol. A 13 (1995) 1426.
[15] W. Hago, D. Kelly, W.H. Weinberg, J. Vac. Sci. Technol. A 14 (1996) 1578.
[16] C.T. Rettner, L.A. DeLouise, D.J. Auerbach, J. Chem. Phys. 85 (1986) 1131.
[17] F. de Jong, A.P.J. Jansen, Surf. Sci. 317 (1994) 1.
[18] G.E. Gdowski, Ph.D. thesis, Stanford University, 1985.
[19] M.P. D'Evelyn, A.V. Hamza, G.E. Gdowski, R.J. Madix, Surf. Sci. 167 (1986) 451.
[20] Y.Z. Barshad, L.S. Bartell, J. Phys. Chem. 92 (1988) 282.
[21] E.J. Valente, L.S. Bartell, J. Chem. Phys. 80 (1984) 1451.
[22] G. Torchet, H. Bouchier, J. Farges, M.F. de Feraudy, B. Raoult, J. Chem. Phys. 81 (1984) 2137.
[23] N. Lee, J.B. Fenn, Rev. Sci. Instrum. 49 (1978) 1269.
[24] D.A. King, M.G. Wells, Surf. Sci. 29 (1972) 454.
[25] J.F. Weaver, M.A. Krzyzowski, R.J. Madix, Surf Sci. 393 (1997) 150.
[26] M.A. Chesters, P. Gardner, Spectrochim. Acta. 46A (1990) 1011.
[27] C.R. Arumainayagam, G.R. Schoofs, M.C. McMaster, R.J. Madix, J. Phys. Chem. 95 (1991) 1041.
[28] J.A. Stinnett, R.J. Madix, J.C. Tully, J. Chem. Phys. 104 (1996) 3134.
[29] J.A. Stinnett, R.J. Madix, J. Chem. Phys. 105 (1996) 1609.
[30] J.A. Stinnett, J.F. Weaver, R.J. Madix, Surf. Sci. 380 (1997) 489.
[31] J.F. Weaver, J.A. Stinnett, R.J. Madix, Surf Sci. 391 (1997) 150.